Proceedings of the
International Conference on Mechanical Engineering 2005
(ICME2005) 28- 30 December 2005, Dhaka, Bangladesh

ICME05-FL-22

EFFECTS OF SURFACE HETEROGENEITY ON THE FLOW FIELD IN ELECTROOSMOTIC FLOW IN MICROCHANNELS UNDER THE DC AND AC ELECTRIC FIELD

Mohammad A. Rahman *

Dalhousie University, Canada.
* marahman@dal.ca

ABSTRACT

The present work is a numerical simulation of electroosmotic flow (EOF) in a cylindrical microchannel with the variation of wall surface charge (ζ -potential) distributions. The 2D Navier-Stoke equation governing the velocity field and the pressure are solved numerically using the finite element method (FEM) The numerical results show that the distorted electroosmotic velocity profiles and various kinds of flow circulation resulting from the axial variation of the ζ . The influences of heterogeneous patterns of zeta potential on the velocity profile, and the induced pressure distribution are discussed in this paper. This study shows that using heterogeneous patterns of zeta potential over the channel can generate local flow circulations and hence provide effective means to improve the mixing within the microchannels. In addition the EOF flow under the AC field enhance the fluid mixing significantly within the entire channel.

Keywords: Electrical double layer, Electroosmotic flow, Microchannel, Surface heterogeneity, Zeta potential.

1. INTRODUCTION

The zeta potential, or potential at the solid-liquid interface is a fundamental parameter in models of electrical double layers (EDL) and their associated properties (electrode capacitance, electroosmosis). The potential applied to an electrode is inherently well defined and easily measured, hence the zeta potential is a natural parameter to use to describe electrochemical properties such as electrode capacitance. Nevertheless, when the same double layer equations are extended for application to electroosmosis, interpretation of the zeta potential becomes much more complicated, since the zeta potential, rather than being straightforwardly controlled by an input voltage, is a result of detailed chemistry and ion distributions at the diffuse interface between substrate and solution [1]. This chemical dependence, combined with the strictly inferential nature of zeta potential measurements, makes it much more difficult to measure and interpret the zeta potential for modeling of electroosmosis [2]. Invariably, zeta potential measurements made in different laboratories do not agree as well as could be expected.

If the channel wall surface is negatively charged, the counter ions in the EDL are positive ions and they will move towards the negative electrode, generating an electroosmotic flow (EOF) in that direction [3]. Transporting liquids in micro channels by applying an electric flied is called electroosmotic flow. Details of the structure of the EDL have historically been of significance to both electrochemistry as well as colloid science, and in-depth reviews on double layer structure can be found in several texts and handbooks [4–9].

The present study adopts a numerical simulation approach to investigate the effects of the continuous and stepwise variation of the zeta potential and the consequent mixing characteristics of 2D electroosmotic flows in the circular microchannels.

2. FORMULATION - GOVERNING EQUATIONS

The microchannel studied here is a cylindrical microchannel with a radius of 50 μm and a length of 300 μm, as shown in Fig. 1. The two ends of the microchannel connect two reservoirs containing the electrodes. When an electrical potential difference is applied to the liquid in the microchannel through these electrodes, electrical driving forces are exerted on the net charges within the EDL. The motion of the net charges will draw the adjacent liquids to move generating electroosmotic flow. The equations governing incompressible liquids flow are the Navier–Stokes equation, and the continuity equation.

$$\rho\left[\frac{\partial\vec{u}}{\partial t}+\vec{u}.\vec{\nabla}\vec{u}\right]=-\vec{\nabla}P+\mu\nabla^2\vec{u}+\vec{E}\rho_e \qquad (1)$$

$$\vec{\nabla}.\vec{u} = 0 \tag{2}$$

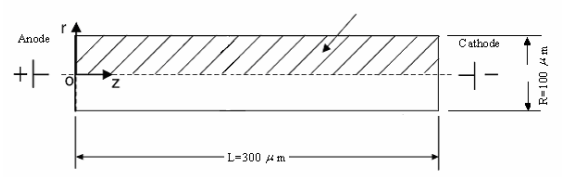

Fig 1. Schematic diagram of the microchannel and the computation domain.

Where, $\vec{u}$ is the velocity vector, μ is the viscosity, ρ is the density of the fluid, $\vec{\nabla}$ P is the pressure gradient (either an induced or an applied pressure gradient), ρ_e is the local net charge density and $\vec{E}$ is the electrical field strength applied to the microchannel. Since the local net charge density is not zero only in the electrical double layer (EDL), the driving force for the electroosmotic flow, $\vec{E}\ \rho_e$, exists only in EDL. The electroosmotic flow velocity changes sharply in a thin layer of liquid near the wall, from zero at the channel wall surface to an approximately constant value at the outer edge of the EDL. For most on-chip microfluidic applications, buffer solutions have a concentration of the order of mM, which results in a very thin EDL. For instance, a solution with a 10 mM concentration has a double layer thickness of approximately 10 nm, which is negligible in comparison with the microchannel diameter (e.g. 100 μm). Therefore, for the purpose of modeling the bulk liquid flow outside the EDL, the driving force term $\vec{E}\ \rho_e$ in Eq. (1) will be dropped off and the electroosmotic effect is considered by the slip boundary condition:

$$\vec{u}_{wall} = \frac{\varepsilon\varepsilon_0\zeta}{\mu}\vec{E} \tag{3}$$

where, μ_{eo} is the electroosmotic mobility of the buffer solution, which will change with zeta potential.

2.1 DC Electric Field

In case of the DC electric field, it can be considered that the flow is steady state, therefore, the transient term in Eq. (1) will be dropped off and Eq. (1) is reduced to:

$$\rho(u_r\frac{\partial u_z}{\partial r} + u_z\frac{\partial u_z}{\partial z}) = -\frac{\partial P}{\partial r} + \mu[\frac{1}{r}\frac{\partial}{\partial r}(r\frac{\partial u_z}{\partial r}) + \frac{\partial^2 u_z}{\partial z^2}] \tag{4}$$

$$\rho(u_r\frac{\partial u_r}{\partial r} + u_z\frac{\partial u_r}{\partial z}) = -\frac{\partial P}{\partial r} + \mu[\frac{1}{r}\frac{\partial}{\partial r}(r\frac{\partial u_r}{\partial r}) + \frac{\partial^2 u_r}{\partial z^2} - \frac{u_r}{r^2}] \tag{5}$$

The flow is axisymmetric and the computation domain as shown in Fig. 1. The corresponding boundary conditions for the velocity component in z-direction are:

$$r = 0, \qquad \frac{\partial u_z}{\partial r} = 0$$

$$r = r_{wall}, \qquad u_z = \mu_{eo}E_z$$

$$z = 0, \qquad \frac{\partial u_z}{\partial z} = 0$$

$$z = z_L, \qquad \frac{\partial u_z}{\partial z} = 0$$

An implication in the above boundary conditions is that at the two ends of the microchannel, the flow patterns are not going through any erupt changes. This condition can be ensured by applying constant zeta potentials near the end of the microchannel, so that any changes in the electroosmotic flow field occur far away from the end boundaries.

The corresponding boundary conditions for velocity component in r-direction are:

$$r = 0, \qquad \frac{\partial u_r}{\partial r} = 0$$

$$r = r_{wall} \qquad u_r = 0$$

Similar to the case with the z-direction boundary conditions, the velocity change along the radial direction at the two end boundaries would be zero:

$$z = 0 \qquad \frac{\partial u_r}{\partial z} = 0$$

$$z = z_{wall}, \qquad \frac{\partial u_r}{\partial z} = 0$$

The pressures at the two ends of the microchannel are generally known, specified as:

$$z = 0, \qquad P = 0$$

$$z = z_L, \qquad P = 0$$

Depending on the applications, P may be the same to simulate an electroosmotic flow, or different to simulate a pressure driven flow or a combined electroosmotic and pressure driven flow. The pressure gradient at the center axis of the microchannel is set to be zero because of symmetric boundary condition, and it was set to be zero at the wall as well considering no flux cross the wall:

$$r = 0, \qquad \frac{\partial P}{\partial r} = 0$$

$$r = r_{wall}, \qquad \frac{\partial P}{\partial r} = 0$$

2.2 AC Electric Field

In case of the AC electric field, the flow is unsteady. Therefore, incorporating the transient term in the N-S equation, Eq. (1) can be written as follows:

$$\rho\left(\frac{\partial u_z}{\partial t}+u_r\frac{\partial u_z}{\partial r}+u_z\frac{\partial u_z}{\partial z}\right)=-\frac{\partial P}{\partial r}+\mu\left[\frac{1}{r}\frac{\partial}{\partial r}\left(r\frac{\partial u_z}{\partial r}\right)+\frac{\partial^2 u_z}{\partial z^2}\right] \quad (6)$$

$$\rho\left(\frac{\partial u_r}{\partial t}u_r\frac{\partial u_r}{\partial r}+u_z\frac{\partial u_r}{\partial z}\right)=-\frac{\partial P}{\partial r}+\mu\left[\frac{1}{r}\frac{\partial}{\partial r}\left(r\frac{\partial u_r}{\partial r}\right)+\frac{\partial^2 u_r}{\partial z^2}-\frac{u_r}{r^2}\right] \quad (7)$$

As a boundary condition, at the inlet and outlet, the relative pressure was set to zero. The electroosmotic velocity given by Eq. 3 was used as a boundary condition. The electric potentials on the two side electrodes are sinusoidal in time with the same maximum value (V) of 0.1 V_{rms} and the same frequency of 8 Hz, but they alternate in polarities. Potentials on the two end electrodes are $V\sin(2\pi ft)$ and $-V\sin(2\pi ft)$ respectively. All other boundaries except the inlet and outlet were assumed to be insulated.

3. NUMERICAL SCHEME

The finite element method (FEM) provides formalism for generating discrete (finite) algorithms for approximating the solutions of differential equations. FEM method is used to solve numerically both the flow field and pressure field distribution of the model described in the previous section. To solve the velocity profile and the pressure gradient of electroosmotic flow in a cylindrical microchannel, the Navier–Stokes equations has been solved in cylindrical coordinate. In order to solve the velocities and other parameters, the pressure gradient at the inlet and the out let has to be known.

4. RESULTS AND DISCUSSION

To simplify the investigation, all results have been obtained using water as the fluid at T = 25 °C. Table 1 summarizes the parameters used, and distinguishes the fixed ones from the varied ones.

Table 1: Chosen Reference Parameters for Simulations for the DC field

Valence of ions	Z	=	1	[-]
Relative dielectric constant	ε	=	78.5	[-]
Dynamic viscosity	μ	=	1×10^{-3}	[kg/ m s]
Absolute temperature	T	=	298	[K]
Capillary radius	R	=	50	[μm]
Capillary length	L	=	300	[μm]
Zeta potential	ζ	=	-20 ~ -120	[mV]
			-50 ~ +50	[mV]
Applied voltage	E_z	=	150	[V]

4.1 Effects on the Distribution of the Heterogeneous Sections

Linear variation of the zeta potential (-20 mV to –100 mV) and the subsequent effects on the flow field and induced pressure field is shown in Figure 2. For a pure electroosmotic flow (without applied pressures) in a channel with a gradual decrease of zeta potential (-20 mV to –100 mV) (Fig. 2(a)) in the axial direction, Fig. 2(b) shows that the plug-like velocity profile is distorted. It is observed that gradual change in velocity occurs with the gradual change in the zeta potential. From the velocity profile, it is observed that the region with –100 mV zeta potential is the active electroosmotic flow (EOF) region; the region with –20 mV zeta potential is the EOF induced flow region. When the liquid in the active EOF region flows downstream, the liquid will pull the liquid in the back (upstream region) due to the continuity. As a result, a negative induced pressure gradient (Fig. 2(b)) is generated to induce the flow in the –20 mV zeta potential region, creating a parabolic velocity profile in the flow direction. Because of the same pressure in the two ends of the microchannel (i.e. open to air), a positive pressure gradient is expected in the active the EOF region, as shown in Fig. 2(d). This induced positive pressure gradient tends to suppress electroosmotic flow, resulting in a distorted electroosmotic velocity profile as shown in Fig. 2(b). This similar distortion has also been observed in a theoretical and experimental study [10]-[11]. If the direction of the variation of zeta potential change is switched, i.e. from −100 mV to –20 mV, the positions of the active EOF region and the EOF induced flow region are switched.

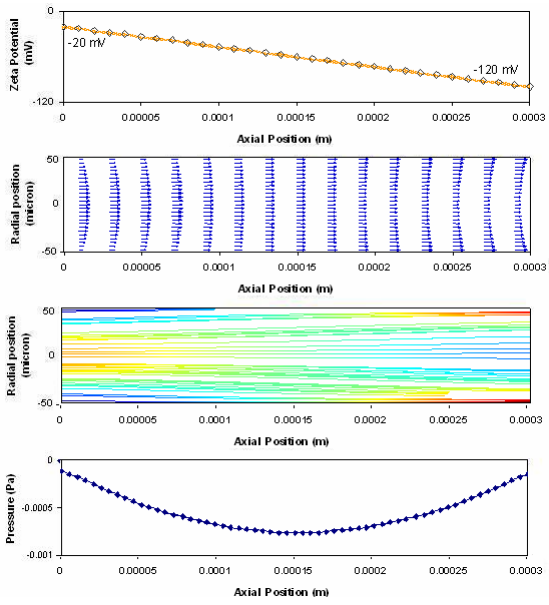

Fig 2. Zeta potential distribution (a) and its corresponding flow field (b), streamlines (c), and pressure field (d) in a 100 μm diameter microchannel under an applied electrical field strength of 0.5 kV/mm in the case of ζ from -20 mV to –100 mV with a linearly deceasing function of equal sized 30 sections

Linear variation of the zeta potential (-50 mV to +50 mV) and consequent effects on the flow field and induced pressure field is shown in Figure 3.

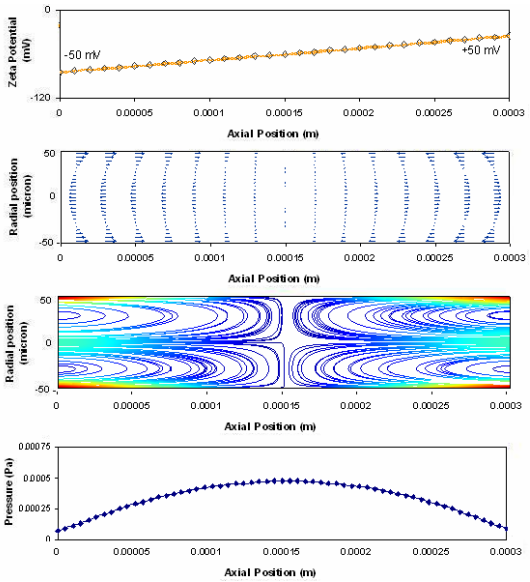

Fig 3. Zeta potential distribution (a) and its corresponding flow field (b), streamlines (c), and pressure field (d) in a 100 μm diameter microchannel under an applied electrical field strength of 0.5 kV/mm in the case of ζ from -50 mV to +50 mV with a linearly increasing function of equal sized 30 sections

For a pure electroosmotic flow (without applied pressures) in a channel with a gradual increase of zeta potential (-50 mV to +50 mV) (Fig. 3(a)) in the axial direction, Fig. 3 shows that the plug-like velocity profile is distorted. It is observed that the liquid in the -50 mV regions wants to flow in the upstream; whereas the liquid in the +50 mV region wants to flow in the downstream. Due to the continuity of the flow, the -50 mV regions create positive pressure gradient inducing the opposite direction flow (upstream). Similarly due to conservation of the continuity of the flow, the +50 mV regions create negative pressure gradient inducing in the opposite direction flow (downstream). The induced positive pressure gradient tends to suppress electroosmotic flow, resulting in a distorted electroosmotic velocity profile as shown in Fig. 3(b). Thus consequent flow separation and flow circulation occurs in the circular microchannel (Fig. 3(c)). With the change of zeta potential from –50 mV to +50 mV, the streamlines in Fig. 3(c) evolves to become recirculatory; the adverse effect such streamlines could have on separation efficiency are obvious. On the other hand, patterning zeta potential in such a way could be quite effective if mixing is desired. A very similar idea was recently explored [12] by computing patterns for in-channel binary fluid "mixers" comprised of solvophobic/solvophilic patches.

The most notable feature in the flow field is that there are back flows, or circulations throughout the microchannel due to the zeta potential change from negative to positive zeta potential. The opposite signs of the zeta potentials indicate opposite EOF driving forces in the two sections of the channel, which provide possibilities of generating circulations. The circulations generated in this case can be seen from the streamline pattern shown in Fig. 3(c). In the region with a positive zeta potential, a negative net charge density exists inside the EDL generating a negative flow towards the anode in the inlet of the channel (the left end). In the region with a negative zeta potential, a positive net charge density exists generating a positive flow towards cathode in the outlet of the channel (the right end).

Variation of the zeta potential from a constant –20 mV (0-100 μm), subsequent linear decrease from -20 mV to –100 mV (100-200 μm) and afterward a constant –100 mV (200-300 μm), is depicted in Fig. 4 (a). Furthermore, the subsequent effects on the flow field, streamlines and induced pressure field are shown in Fig 4 (b)-(d).

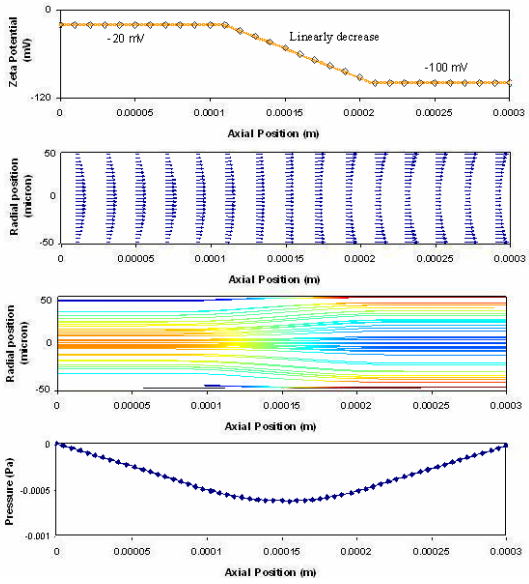

Fig 4. Zeta potential distribution (a) and its corresponding flow field (b), streamlines (c), and pressure field (d) in a 100 μm diameter microchannel under an applied electrical field strength of 0.5 kV/mm in the case of ζ from a constant of -20 mV to a linearly deceasing function to a constant of –100 mV.

Fig. 4 shows a more complicated zeta potential pattern and its corresponding flow field and pressure field. In this case, the induced pressure gradient is nonlinear through the microchannel, as shown in Fig. 4(b). The induced pressure gradient is higher compared to the previous section where there was a linear decrease of the zeta potential from –20 mV to –100 mV. For the regions with –20 mV potentials, negative pressure gradients exist to accelerate the flow, compensating the smaller EOF driving force in this region. For the regions with –100 mV zeta potentials, positive pressure gradients present to against high-speed electroosmotic flow in this region. As a result, modified positive parabolic velocity profiles in the –20 mV zeta potential regions and modified negative parabolic velocity profiles in the –100 mV zeta potential regions are observed, as shown in Fig. 4(b). Between the channel length 100-200 μm (linearly

deccrease from –20 mV to -100 mV) transition occurs from modified positive parabolic velocity profiles to modified negative parabolic velocity profiles

Variation of the zeta potential from a constant –50 mV (0-100 μ m), subsequent linear increase from -50 mV to +50 mV (100-200 μ m) and afterward a constant +50 mV (200-300 μ m), is depicted in Fig. 5 (a). Furthermore the consequent effects on the flow field streamline and induced pressure field is shown in Fig 5 (b)-(d).

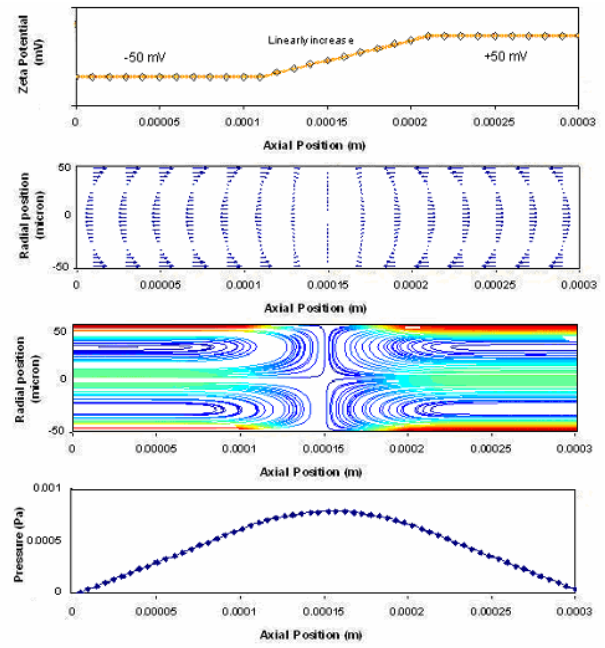

Fig 5. Zeta potential distribution (a) and its corresponding flow field (b), streamlines (c), and pressure field (d) in a 100 μ m diameter microchannel under an applied electrical field strength of 0.5 kV/mm in the case of ζ from a constant of -50 mV to a linearly increasing function to a constant of +50 mV.

Fig. 5 shows a more complicated zeta potential pattern and its corresponding flow field and pressure field. In this case, the induced pressure gradient is nonlinear through the microchannel, as shown in Fig. 5(b). The induced pressure gradient is higher compared to the previous section where there was a linear increase of the zeta potential from –50 mV to +50 mV. For the regions with –50 mV potentials, positive pressure gradients exist to decelerate the flow. For the regions with +50 mV zeta potentials, negative pressure gradients present favor of high-speed electroosmotic flow in this region. As a result, modified negative parabolic velocity profiles in the –50 mV zeta potential regions and modified positive parabolic velocity profiles in the +50 mV zeta potential regions are observed, as shown in Fig. 5(b). Between the channel length 100-200 μ m (linearly increase from –50 mV to +50 mV) transition occurs from modified negative parabolic velocity profiles to modified positive parabolic velocity profiles. As shown in Fig. 5 (c) the flow separation and consequent flow circulation occurs.

As shown in Fig. 5 (c), there are back flows, or circulations throughout the microchannel due to the oppositely charged channel wall surfaces in the two sections. In the region with a positive zeta potential, a negative net charge density exists inside the EDL generating a negative flow towards the anode in the inlet of the channel (the left end). In the region with a negative zeta potential, a positive net charge density exists generating a positive flow towards cathode in the outlet of the channel (the right end). It was found that the net flow direction depends on the overall strength of the zeta potential. The overall zeta potential strength is zero in this case and indicates no net flow (in z-direction), as shown in Fig. 5(b) and (c). As a result of these opposite migrations of ions, the magnitude of both positive and negative pressure gradients are higher than that in the previous cases. Clearly, such flow behavior can be used to enhance the flow mixing.

4.2 AC Field

The finite element (FEM) method was used to solve numerically both the AC electrical field and corresponding flow field of the model described in the previous section. The electric potentials on the two side electrodes are sinusoidal in time with the same maximum value (V) of 0.1 V_{rms} and the same frequency of 8 Hz, but they alternate in polarities. Potentials on the two end electrodes are Vsin(2πft) and -Vsin(2πft) respectively. Values used for time dependent simulation is presented in Table 2.

Table 2: Chosen Reference Parameters for Simulations for the AC field

Conductivity of the ionic solution	σ	=	0.11845	[S]
Frequency of the AC potential	f	=	8	[1/s]
Angular frequency	ω	=	$2\pi f$	[rad/s]
Absolute temperature	T	=	298	[K]
Capillary radius	R	=	50	[μm]
Capillary length	L	=	300	[μm]
Zeta potential	ζ	=	-20 ~ -120	[mV]
			-50 ~ +50	[mV]
Maximum value of the AC potential	V	=	0.1	[V]

As shown in Fig. 6, at t=0.025 sec fluid flow direction is in upstream way and at t=0.075 sec the overall fluid flow in the channel is in the downstream direction. The physical explanation of the flow field is discussed in the previous sections. Potentials on the two end electrodes are Vsin(2πft) and -Vsin(2πft) respectively. The above-mentioned flow characteristic is occurred, as the electric potentials on the two side electrodes are sinusoidal in time but they alternate in polarities. This

flow behavior enhance the fluid mixing significantly. Most interesting flow direction is observed at time t=0.125 sec. At this time fluid flow occurs in the same direction within the entire channel length. After this time the cycles repeats again.

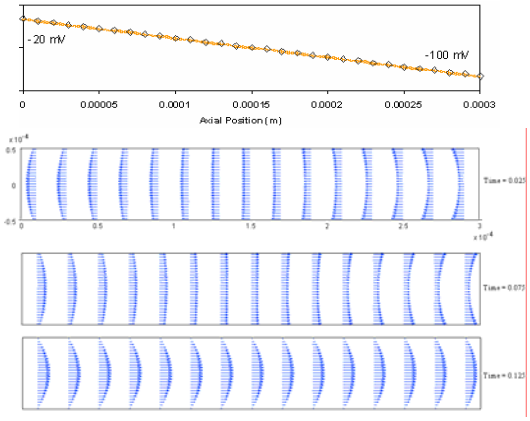

Fig 6. Transient development of the velocity vector over 0.125 sec. In this case the zeta potential varies from –20 mV to –100 mV along the z direction of the channel.

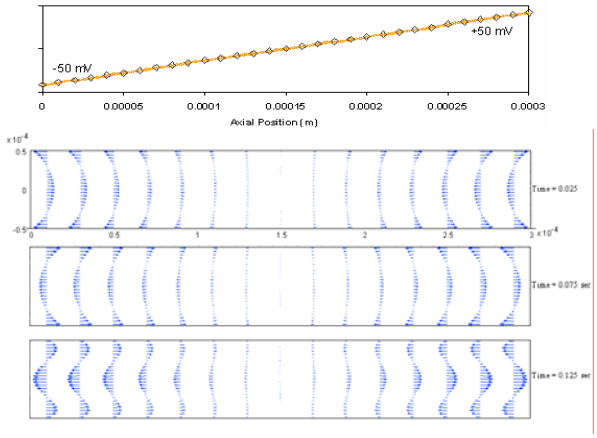

Fig 7. Transient development of the velocity vector over 0.125 sec. In this case zeta potential varies from –50 mV to +50 mV along the z direction of the channel.

As shown in Fig. 7, at t=0.025 sec fluid flow inwards from the two end sections of the channel, and at t=0.075 sec and t=0.125 sec the overall fluid flow directs in the outward direction towards the both end. The physical expiation of the flow field is discussed in the previous sections.

5. CONCLUSIONS

This paper presents a numerical simulation of the EOF in cylindrical microchannel with a continuous and stepwise variation of the ζ change along the microchannel. The results show that the different types of velocity profiles in the upstream and the downstream sections can be generated by the variation of the ζ distribution. It was observed that change in the ζ from –20 mV to –100 mV cannot generate flow circulation as in this case the zeta potential change does not involve the sign change of the surface charge. On the other hand, change in the ζ from –50 mV to +50 mV can generate flow circulation as in this case the zeta potential change involves the sign change of the surface charge. Several heterogeneous patterns involving zeta potential changes from positive to negative or negative to positive have been investigated to explore the optimum distribution that can be able to generate different types of flow circulations which can be observed from the streamlines. The adverse effect such streamlines could increase the separation phenomena. On the other hand, patterning zeta potential in such a way could be quite effective if mixing is desired. Mixing would be enhanced for a series of small heterogeneous patches (with sign change of the ζ) rather than a long single patch, due to the degree of velocity disruption over this region. Furthermore, the EOF flow under the AC field enhances the fluid mixing significantly within the entire channel.

6. REFERENCES

1. Yang, R.J., Fu, L.M. and Lin, Y.C., 2001, J. Colloid Interface Sci., 236 : 98-105.
2. Long, D., Stone, H.A. and Ajdari, A., 1999, J. Colloid Interface Sci., 212 : 338-349
3. Li, D., 2004, *Electrokinetics in Microfluidics*, Academic Press, NY.
4. Hunter, R.J., 1989, *Foundations of Colloid Science*, Clarendon Press, Oxford, vol. 2.
5. Lyklema, J.H., 1991, *Fundamentals of Interface and Colloid Science*, Academic Press, London.
6. Kralchevsky, P.A., Danov, K.D., Denkov, N.D., Birdi K.S. (Eds.), 2003, *Handbook of Surface and Colloid Chemistry*, CRC Press, Boca Raton, FL, p.137.

7 Gileadi, E., Kirowa, E., Penciner, J., 1975, *Interfacial Electrochemistry: An Experimental Approach*, Addison-Wesley, Reading, MA.

8. Overbeek, J.T.G.., 1952, *Colloid Science*, Elsevier, Amsterdam, vol. 1.
9. Bard, A.J., Faulkner, L.R., 2001, *Electrochemical Methods: Fundamentals and Applications*, Wiley, New York.
10. Herr, A.E., Molho, J.I., Santiago, J.G., Mungal, M.G., Kenny, T.W., 2003, Anal. Chem., 72 :1053.
11. Lee, S.H.J., Ren, L.C., Li, D., 2005, Anal. Chim. Acta, 530 : 273–282.
12. Kuksenok, O., Yeomans, J.M., Balazs, A.C., 2001, Langmuir, 17 : 7186–7190.